Research article

Ethanolic extract of *Ocimum sanctum* leaf modulates oxidative stress, cell cycle and apoptosis in head and neck cancer cell lines

Kusumawadee Utispan [a,*], Sittichai Koontongkaew [b], Nattisa Niyomtham [b], Boon-ek Yingyongnarongkul [c]

[a] *Faculty of Dentistry, Thammasat University, Pathum Thani, 12120, Thailand*
[b] *Walailak University International College of Dentistry, Walailak University, Bangkok, 10300, Thailand*
[c] *Department of Chemistry and Center of Excellence for Innovation in Chemistry (PERCH-CIC), Faculty of Science, Ramkhamhaeng University, Bangkok, 10240, Thailand*

A R T I C L E   I N F O

A B S T R A C T

Ocimum sanctum Linn. is a medicinal herb that has cytotoxic effects by inducing oxidative stress in some carcinomas. This study aimed to examine the impact of *O. sanctum* leaf extract on oxidative stress, cell cycle progression, and apoptosis in cell lines of head and neck squamous cell carcinoma (HNSCC). Isogenic primary (HN18/HN30) and metastatic (HN17/HN31) HNSCC cell lines were used. Preparation of the ethanolic extract of *O. sanctum* leaf (EEOS) was carried out. HNSCC cell lines were exposed to varying concentrations (0.1–0.8 mg/ml) of EEOS for a duration of 72 h, and the MTT assay was utilized to determine the cytotoxic doses. To assess the impact of EEOS on HNSCC cells, the levels of reactive oxygen species (ROS) and malondialdehyde were measured using a fluorometric method. Flow cytometry was utilized to evaluate effects of EEOS on the cell cycle, DNA damage, and apoptosis in HNSCC cells. Caspase-3 and -9 levels in the EEOS-treated HNSCC cells were measured by ELISA. The chemical components in EEOS were detected using high-performance liquid chromatography-electrospray ionization-time of flight-mass spectrometry. EEOS exhibited cytotoxicity against the HN18, HN17, HN30 and HN31 cells at minimum concentrations of 0.1, 0.3, 0.2 and 0.2 mg/ml, respectively. Treatment with EEOS resulted in a significant increase in ROS levels in HN18 and HN17 cells. Additionally, EEOS significantly induced the levels of malondialdehyde in HN18 and HN31 cells. Moreover, EEOS arrested the cell cycle in HN30 and HN31 cells, and significantly induced DNA damage and apoptosis in the HN18, HN30, and HN31 cells. EEOS selectively increased caspase-9 in the HN18 cells. However, caspase-3 was activated without apoptosis in the EEOS-treated HN17 cells. The constituents of EEOS were identified as rosmarinic acid, caffeic acid, and apigenin. In conclusion, EEOS exhibits various prooxidative and apoptotic effects between HNSCC cells.

1. Introduction

Head and neck squamous cell carcinoma (HNSCC) is a term used to describe cancers that originate from the mucosal squamous epithelial cells in the oral cavity and pharynx. Head and neck cancer is the seventh most common human malignancy worldwide [1].

---

* Corresponding author.
   E-mail address: kusumawadee.utispan@gmail.com (K. Utispan).

Despite advances in treatment options, the five-year survival rate for HNSCC has not shown significant improvement over the past decade, which can be attributed to the resistance of cancer cells to therapy [2]. Radiation and chemotherapy drugs are commonly used for treating HNSCC. These therapeutic regimens affect the cancer cells by increasing reactive oxygen species (ROS) levels [3]. Natural herbs such as curcumin, quinones, quercetin, and terpenoid have been shown to be effective in regulating ROS levels in head and neck cancer cells, and have the potential to enhance the efficacy of conventional chemo-/radiotherapy [4]. Moreover, emerging interdisciplinary techniques such as photodynamic [5] and nanoparticle systems [6] provide additional options for regulating ROS levels in head and neck cancer, in conjunction with chemo-/radiotherapy.

Free radicals, including ROS and reactive nitrogen species (RNS), are implicated in the pathogenesis of several cancers, including HNSCC [7]. During the oxidative metabolism of the cancer cells, free radicals are produced. Upregulation of ROS can increase malondialdehyde, that can cause lipid peroxidation and DNA damage, and ultimately lead to cell death. Basal levels of ROS maintain homeostasis in normal cells. Increased levels of ROS affect a variety of tumor activities depending on the ROS concentration. Chronic oxidative stress can lead to low concentrations of ROS, which promote cell mitosis and increase genomic instability. On the other hand, moderate concentrations of ROS can cause temporary or permanent cell cycle arrest [8]. Moreover, high ROS concentrations promote acute oxidative stress by damaging macromolecules and inducing apoptosis, necrosis, and ferroptosis. Therefore, ROS upregulation during chemo-/radiotherapy is toxic to tumor cells. Despite regulating ROS levels have potential benefits in cancer therapy, it should be noted that high levels of ROS can also promote multidrug resistance in cancer cells during chemotherapy, which can significantly limit the efficacy of cancer treatment and impact the quality of life of patients [9]. Natural herbs are one possible option for regulating ROS levels in cancer therapy, including strategies to increase ROS levels. Various phytochemical constituents found in natural herbs, including flavonoids [10,11], polyphenols [12], and quinones [13], have been utilized in the comprehensive treatment of HNSCC by increasing ROS levels.

Ocimum sanctum Linn., commonly known as "Holy basil" [14], is a native medicinal herb and is grown throughout eastern Asian countries, including Thailand [15,16]. *O. sanctum* contains phytochemicals as a major chemical component. The composition of phytochemicals in this plant is subject to variations based on factors like growing conditions, harvesting methods, and extraction techniques [17]. The extracts obtained from the leaves and stem of the plant have been found to contain various phenolic compounds and flavonoids [18]. In recent studies, it has been shown that *O. sanctum* exhibits a variety of biological and pharmacological activities, such as antioxidant [19,20], anti-inflammatory [21], antimicrobial [22], and anticancer effects [17], which are attributed to the presence of phytochemical compounds in different parts of the plant such as leaves, stems, roots, flowers, and seeds.

The ethanolic extract of *O. sanctum* (EEOS) leaf has been demonstrated to have anticancer effects on several human tumors, e.g. gastric [20], pancreatic [23], non-small cell lung [24], and head and neck cancer [25,26]. Moreover, the EEOS exerts its anticancer activities by promoting cancer cell apoptosis and cell cycle arrest, increasing lipid peroxidation and cytotoxicity, and inhibiting cell invasion, angiogenesis, and metastasis [20,23–26].

Previous studies using natural extracts in the reported cancer models suggested that EEOS might be used as part of comprehensive cancer treatment by promoting oxidative stress [10,12,13]. To date, there have been no reports on the impact of EEOS on oxidative stress in HNSCC cells. Therefore, the objective of this study was to investigate the impact of EEOS on oxidative stress in HNSCC cells by assessing ROS levels and examining its subsequent effects on lipid peroxidation, DNA damage, cell cycle, apoptosis, and levels of caspase-9 and 3 in the treated cell lines.

2. Materials and methods

2.1. Chemical reagents

Acetonitrile and water (HPLC grade) were purchased from Fisher Scientific (Pittsburgh, PA, USA). Ethanol and methanol (analytical grade) were purchased from Merck (Darmstadt, Germany). Caffeic acid, rosmarinic acid, and apigenin were purchased from Sigma-Aldrich (St. Louis, MO, USA).

2.2. EEOS preparation

The *O. sanctum* leaves were collected as previously described [25]. The *O. sanctum* leaves were prepared and extracted in ethanol as previously described [25]. The EEOS powder was kept at 4 °C until used.

2.3. Cell culture and treatments

Professor Silvio Gutkind, from the Moores Cancer Center in the Department of Pharmacology at UCSD, provided the isogenic HNSCC cell lines representing primary and metastatic sites from the same patient, which were initially established by Ensley J [27]. The HN18 cells were obtained from primary tongue lesions and the HN17 cells were taken from neck dissections (T2N2M0 stage). The HN30 cells were obtained from primary pharynx lesions and the HN31 cells were taken from lymph node metastases (T3N1M0 stage). The cells were cultured in Dulbecco's Modified Eagle's medium (DMEM) (Invitrogen, Carlsbad, CA, USA) supplemented with 10% fetal bovine serum (FBS), 100 U/ml penicillin, and 100 μg/ml streptomycin in a 5% CO_2 atmosphere at 37 °C. The EEOS was dissolved in dimethyl sulfoxide (DMSO), and then diluted in DMEM containing 10% FBS to 0.1, 0.2, 0.3, 0.4, 0.5, 0.6, 0.7, and 0.8 mg/ml EEOS. The final concentration of DMSO in the media was 0.4%.

2.4. Cytotoxicity assessment

The cell viability was measured by a 3–4,5-Dimethylthiazol-2-yl-2,5-Diphenyltetrazolium Bromide (MTT) assay after a 72 h exposure as previously described [25]. Briefly, the cells were seeded in 96-well plates at 5000 cells/well and cultured for 24 h. Cells were treated with 0.1, 0.2, 0.3, 0.4, 0.5, 0.6, 0.7, or 0.8 mg/ml EEOS for 72 h. Cells cultured in 10% FBS-DMEM or 0.4% DMSO were used as controls. After treatment, 50 μl MTT (Sigma) (2 mg/ml) was added to each well and incubated for 4 h. To determine the cell viability, the formazan crystals that indicated the presence of viable cells were dissolved in DMSO and measured at 570 nm using a microplate reader (Tecan, Salzburg, Austria). The percentage of viable cells in the treatment groups was calculated in comparison to the control group. This was done using the following formula: cell viability (%) = (mean Abs570 treated cells - mean Abs570 blank)/(mean Abs570 control cells - mean Abs570 blank) × 100. Each concentration of EEOS was tested three times in three independent experiments. The minimum EEOS concentration that significantly reduced the % cell viability was defined as the cytotoxic concentration of EEOS. The cytotoxic concentration on each individual cell line was used in the subsequent experiments.

The IC_{50} (the half maximal inhibitory concentration) values were calculated with nonlinear regression, log (inhibitor) vs. response (four parameters) for each HNSCC cell line.

2.5. Intracellular ROS levels determination

The cells were seeded in 96-well black plates (Merck) at 20,000 cells/well and incubated for 24 h. The minimum cytotoxic concentration of EEOS on the HN18, HN17, HN30, and HN31 cells was 0.1, 0.3, 0.2, and 0.2 mg/ml, respectively. These concentrations were used to treat the cells for 24 h. The cells' intracellular ROS level were determined using 2′,7′- dichlorofluorescin diacetate (DCFDA) in a ROS detection assay kit (Abcam, Waltham, MA, USA) per the manufacturer's instructions. The intracellular ROS converted DCFDA to 2′,7′- dichlorofluorescin and the fluorescent signal was detected using an excitation/emission spectra of 495/529 nm in a fluorescence microplate reader (Thermo Fisher Scientific, Waltham, MA USA). Each EEOS treatment was performed in three independent experiments.

2.6. Malondialdehyde adduct determination

The cells were seeded in 6-well plates at 500,000 cells/well and incubated for 24 h. The HN18, HN17, HN30, and HN31 cells were then treated with 0.1, 0.3, 0.2, and 0.2 mg/ml EEOS, respectively, for 24 h. The cells were lysed by the malondialdehyde lysis solution in a lipid peroxidation malondialdehyde assay kit (Abcam). The cell lysate was centrifuged at 13,000×g for 10 min, and the supernatant was collected. The malondialdehyde adduct produced by the lipid peroxidation reaction was determined in the supernatant following the manufacturer's instructions. The malondialdehyde was measured using an excitation/emission spectra (532/553) nm in a fluorescence microplate reader (Thermo Fisher Scientific). The malondialdehyde adduct in the EEOS-treated cell or control was quantified using a malondialdehyde standard curve. Three independent EEOS treatments were performed.

2.7. Cell cycle and DNA damage analysis

The cells were sub-cultured into 6-well plates at 500,000 cells/well for 24 h. The cells were then synchronized at the G1 phase of the cell cycle by culturing them in serum-free DMEM for 24 h. After G1 phase synchronization, the HN18, HN17, HN30, and HN31 cells were treated with 0.1, 0.3, 0.2, and 0.2 mg/ml EEOS, respectively, for 24 h. Cells in 10% FBS-DMEM or 10 μg/ml cisplatin (Sigma) were used as controls. The cells were prepared and the cell cycle was analyzed as previously described [28]. Briefly, the EEOS-treated cells or control were trypsinized, centrifuged at 200×g for 5 min, and the cell pellets were collected. To eliminate RNA, the cell pellets were incubated with 10 μg/μl DNase-free RNaseA (USB Corporation, Cleveland, OH, USA) at 37 °C for 30 min. The DNA was stained with 1 mg/ml propidium iodide (Sigma) for 15 min at 4 °C with light protection. The percentage of cells in individual stage of the cell cycle was analyzed in a flow cytometer and CytExpert software (Cytoflex®, Beckman Coulter, Indianapolis, IN, USA). The percentage of cells in the G0/G1 phase of the cell cycle was measured and compared between conditions with and without EEOS treatment. DNA damage was determined by the percentage of cells in the sub-G1 phase of the cell cycle and compared between conditions with and without EEOS treatment.

2.8. Apoptosis detection

The cells were seeded in 6-well plates at 500,000 cells/well for 24 h. After adhesion, the HN18, HN17, HN30, and HN31 cells were treated with 0.1, 0.3, 0.2, and 0.2 mg/ml EEOS, respectively, for 24 h. Cells in 10% FBS-DMEM or 10 μg/ml cisplatin were used as controls. The cells were prepared and stained with annexin-V- fluorescein isothiocyanate (FITC) and 7-amino-actinomycin D (7-AAD) using an apoptosis assay kit (BioLegend, San Diego, CA, USA) according to the manufacturer's instructions. The number of viable, and early/late apoptotic cells was counted in a flow cytometer using CytExpert software (Cytoflex®, Beckman Coulter). The percentage of apoptotic cells was measured and compared between conditions with and without EEOS treatment.

2.9. Caspase-9 and -3 determination

The cells were maintained in 6-well plates at 500,000 cells/well for 24 h. The HN18, HN17, HN30, and HN31 cells were then
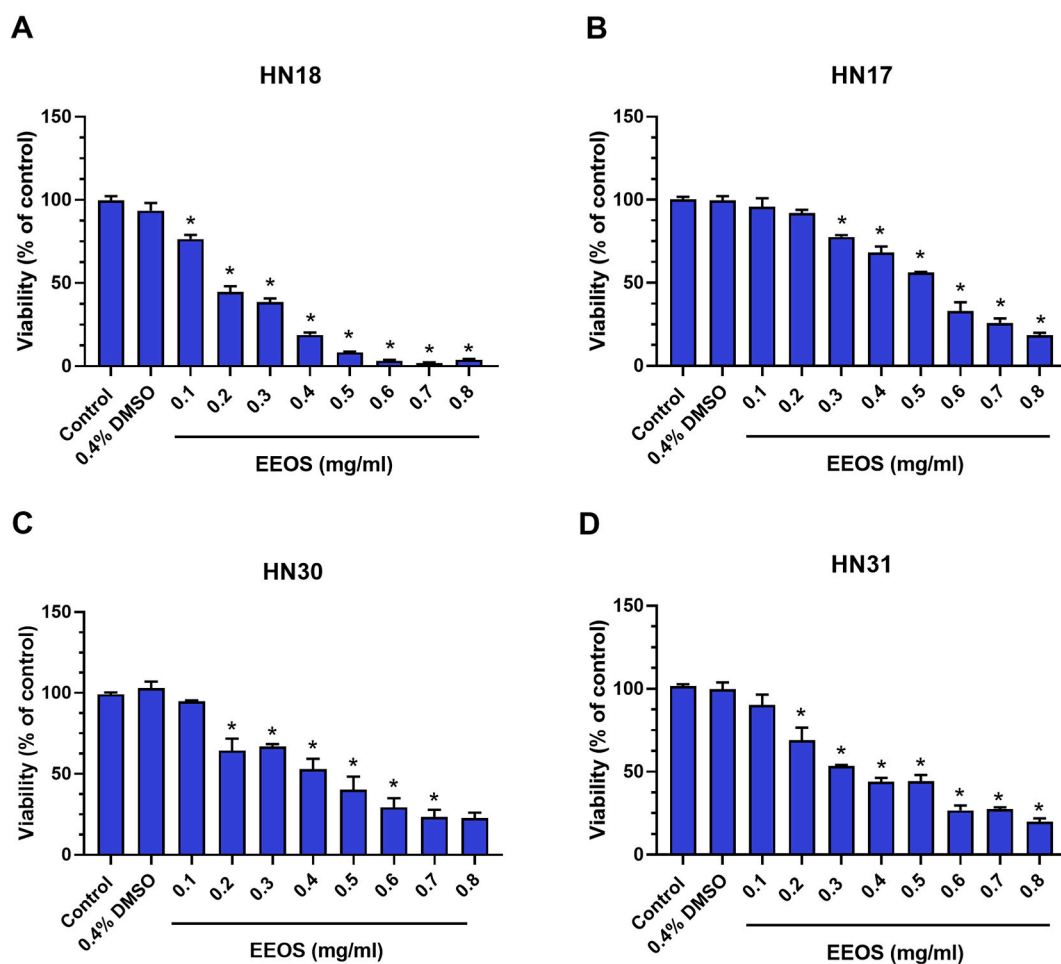
Fig. 1. Cytotoxicity test of EEOS on HNSCC cell lines. The EEOS or 0.4% dimethyl sulfoxide (DMSO) were used to treat the (A) HN18, (B) HN17, (C) HN30 and (D) HN31 cells for 72 h. Cell viability was measured by an MTT assay. Bars represent the mean $\pm$ standard error of percentage of cell viability. *$p < 0.05$ vs control.

treated with 0.1, 0.3, 0.2, and 0.2 mg/ml EEOS, respectively, for 24 h. Cells in 10% FBS-DMEM served as a control. The cells were lysed and caspase-9 and -3 were detected using caspase-9 and caspase-3 Human ELISA kits (Abcam), respectively, as per the manufacturer's instructions. Briefly, the cell lysate and the antibody cocktail for caspase-9 or caspase-3 active forms were added to each well in a microplate strip. The microplate strip was incubated at room temperature for 1 h. The unbound antibody was washed off, and the antigen-antibody signal was developed by the TMB development solution. The activated caspase-9 or caspase-3 level was measured at 450 nm in a microplate reader (Tecan). The fold change in caspase-9 and -3 was normalized to the control.

2.10. HPLC-ESI-TOF-MS analysis of EEOS

To analyze the chemical compounds, present in EEOS, high-performance liquid chromatography coupled with electrospray ionization-time of flight-mass spectrometry (HPLC-ESI-TOF-MS) was used. EEOS was first diluted in methanol to a concentration of 1 mg/ml and then filtered through a 0.45 μm membrane filter. The resulting solution was then injected into an UltiMate® 3000 HPLC system (Thermo Fisher Scientific). Caffeic acid, rosmarinic acid, and apigenin were used as standard polyphenolic compounds for this analysis. Caffeic acid (0.5, 0.75, 1, 2.5, 5, 7.5, and 10 μg/ml), rosmarinic acid (2.5, 5, 7.5, 10, 12.5, 15, 17.5, and 20 μg/ml), and apigenin (0.1, 0.25, 0.5, 0.75, 1, 1.25, and 1.5 μg/ml) were prepared in methanol. HPLC was performed using a reverse phase column (Symmetry C18 analysis column, 2.1 mm × 150 mm, and 3 μm particle size) (Thermo Fisher Scientific) at 40 °C. The gradient mobile phase system consisted of HPLC water (Component A) and acetonitrile (Component B). Elution was performed at a 0.3 ml/min flow rate. The program of gradient elution was: 5–15% B (0–10 min), 15–95% B (10–30 min), and 5% B (30–35 min). An injection volume of 2 ml was used, and the components separated by the HPLC were analyzed mass to charge ratio (m/z) in an ESI-TOF-MS system (micrOTOF-Q-II, Bruker Daltonics, Bremen, Germany). The ESI system operated in negative-ion mode, generating m/z values in the range 50–1000. The mass spectrometric conditions were optimized with a gas temperature of 200 °C, drying gas flow rate of 8 l/min, nebulizer gas pressure of 2 bar, and a capillary potential of 3000 V. The phenolic components in EEOS were quantitatively determined
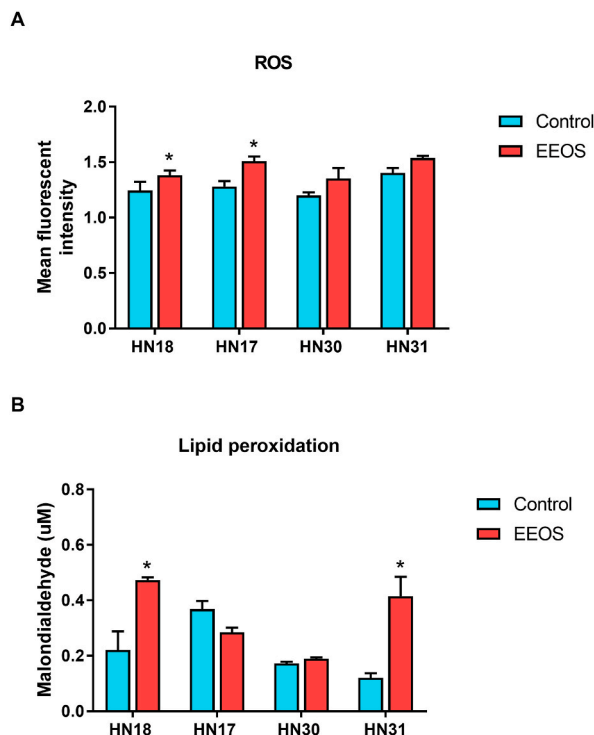
A

ROS

B

Lipid peroxidation

Fig. 2. Determination of the intracellular ROS and lipid peroxidation in EEOS-treated HNSCC cells. The HN18, HN17, HN30, and HN31 cells were treated with 0.1, 0.3, 0.2, and 0.2 mg/ml EEOS, respectively. A) The mean fluorescent intensity representing ROS in the EEOS-treated cells was determined using a DCFDA-based ROS detection assay. B) Lipid peroxidation in the EEOS-treated cells was investigated by quantifying the malondialdehyde adduct. Bars represent the mean ± standard error of fluorescence intensity or malondialdehyde concentration. $*p < 0.05$ vs. control.

using a standard calibration curve. The data were analyzed using Bruker Compass Data Analysis 4.0 software (Bruker Daltonik).

2.11. Statistical analysis

The cell viability percentage was calculated. The mean IC_{50} and 95% confidence interval values were determined by non-linear regression. The normal distribution of the data was tested by the Shapiro-Wilk test [29]. The results are presented as means and standard error. Because the data had a normal distribution, multiple group comparisons were performed using one-way ANOVA followed by Dunnett's post hoc test. The mean differences between the two groups were analyzed by the unpaired *t*-test. Statistical analyses were performed using Prism GraphPad 7.04 software (GraphPad Software, La Jolla, CA, USA). Statistically significant was considered when $p \leq 0.05$.

3. Results

3.1. Cytotoxicity of EEOS on HNSCC cells

The EEOS was dissolved in 0.4% DMSO and diluted to 0.1, 0.2, 0.3, 0.4, 0.5, 0.6, 0.7, and 0.8 mg/ml and then tested for its toxicity on the HNSCC cell lines. The data demonstrated no significant differences in cell viability between the 0.4% DMSO and medium control groups ($p > 0.05$) (Fig. 1). The HN18 cell viability was significantly decreased in the 0.1–0.8 mg/ml EEOS groups compared with the control group ($p < 0.05$) (Fig. 1A). At 0.3–0.8 mg/ml EEOS, the HN17 cells demonstrated significantly reduced viability compared with control ($p < 0.05$) (Fig. 1B). Moreover, 0.2–0.8 mg/ml EEOS significantly reduced HN30 and HN31 cell viability compared with control ($p < 0.05$) (Fig. 1C and D). The IC_{50} value of the EEOS 72 h-treatment was calculated to be 226 µg/ml (95%CI: 222–231 µg/ml) for the HN18 cells, 262 µg/ml (95%CI: 259–265 µg/ml) for the HN17 cells, 246 µg/ml (95%CI: 238–254 µg/ml) for the HN30 cells, and 238 µg/ml (95%CI: 232–243 µg/ml) for the HN31 cells. The minimum significant cytotoxic concentration for the individual cell line was applied in subsequent experiments. The minimum cytotoxic concentration of EEOS for the HN18, HN17, HN30, and HN31 cells was 0.1, 0.3, 0.2, and 0.2 mg/ml, respectively.
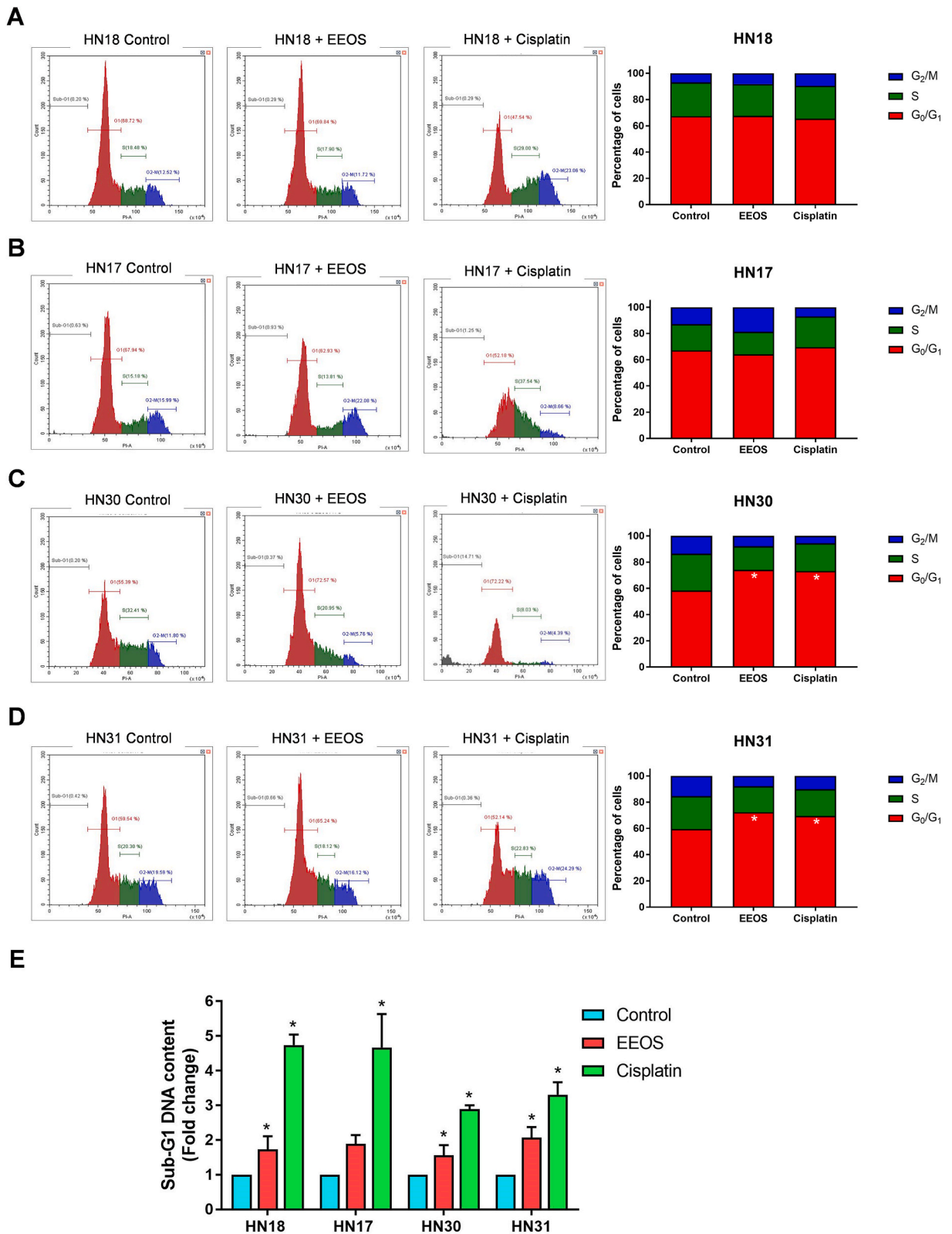
(caption on next page)

Fig. 3. EEOS induced cell cycle arrest and DNA damage in HNSCC cells. EEOS at a minimum cytotoxic concentration of 0.1, 0.3, 0.2 and 0.2 mg/ml was used to treat the HN18, HN17, HN30, and HN31 cells, respectively. Cisplatin (10 μg/ml) was used as the positive control. The histogram and stacked bar graphs display the cell cycle status in the EEOS-treated (A) HN18, (B) HN17, (C) HN30 and (D) HN31 cells. E) The DNA damage in the EEOS-treated cells was determined at the sub-G1 phase of the cell cycle. Bars represent the mean ± standard error of DNA damage fold change normalized to the control. *$p < 0.05$ vs control.
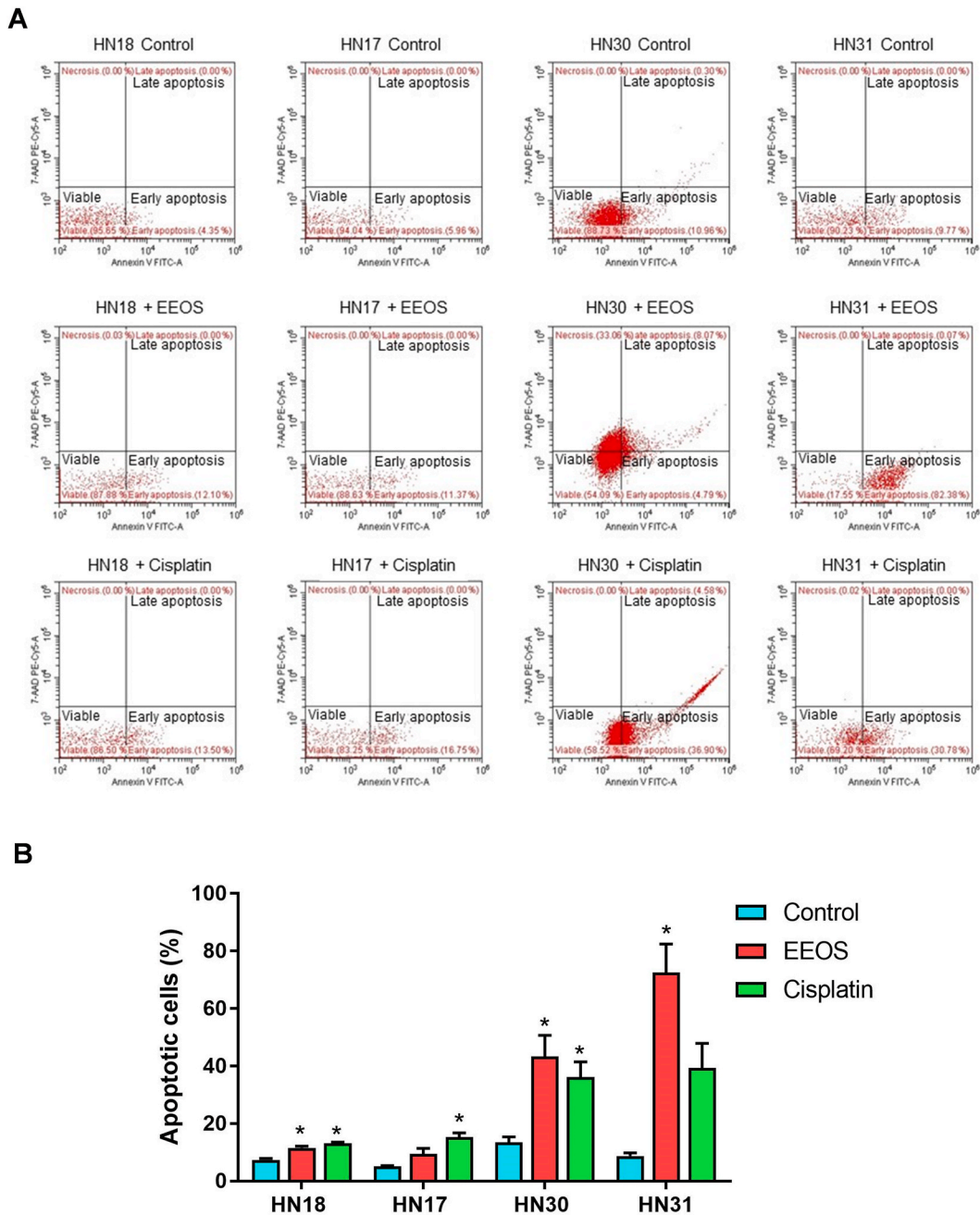

Fig. 4. Detection of apoptosis in EEOS-treated HNSCC cells. EEOS at a minimum cytotoxic concentration of 0.1, 0.3, 0.2, and 0.2 mg/ml was used to treat the HN18, HN17 and, HN30, and HN31 cells, respectively. Cisplatin (10 μg/ml) was used as the positive control. A) Scatter-plot diagram of flow cytometric analysis displays the apoptotic status of the HNSCC cells treated with EEOS or cisplatin. B) Total apoptotic cells were quantified in the EEOS or cisplatin treatment. Bars represent the mean ± standard error of the percentage of apoptotic cells. *$p < 0.05$ vs control.
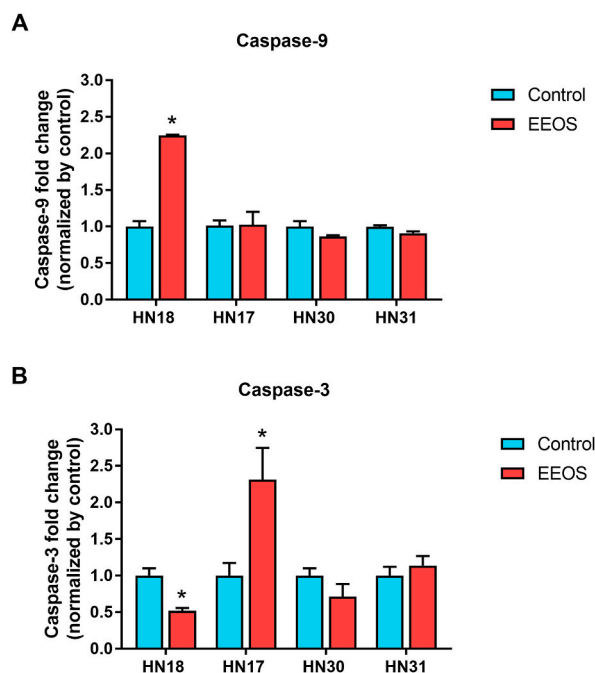
Fig. 5. Determination of activated caspase-9 and -3 levels in the EEOS-induced HNSCC cells. EEOS at a minimum cytotoxic concentration of 0.1, 0.3, 0.2, and 0.2 mg/ml was used to treat the HN18, HN17, HN30, and HN31 cells, respectively. The EEOS-induced cells were evaluated for (A) caspase-9, and (B) −3 levels. Bars represent the mean ± standard error of caspases fold change normalized to the control. *$p < 0.05$ vs control.

3.2. Effect of EEOS on oxidative stress in HNSCC cells

Excessive generation of ROS can trigger oxidative stress and lead to lipid peroxidation. The intracellular ROS level and lipid peroxidation-produced malondialdehyde served as representative oxidative stress markers in the EEOS-treated cells. The HN18 and HN17 cells were cultured with 0.1 and 0.3 mg/ml EEOS, respectively. The results revealed that the ROS mean fluorescent intensity (MFI) significantly increased in the EEOS-treated HN18 and HN17 groups compared with control ($p < 0.05$) (Fig. 2A). In contrast, the ROS MFI in the 0.2 mg/ml EEOS-treated HN30 and HN31 groups showed no significant change compared with control ($p > 0.05$). A significantly increased malondialdehyde concentration was observed in the EEOS-treated HN18 and HN31 groups compared with control ($p < 0.05$) (Fig. 2B). In contrast, EEOS did not induce lipid peroxidation in the HN17 and HN30 groups.

3.3. Effect of EEOS on cell cycle and DNA damage in HNSCC cells

EEOS at the minimum cytotoxic concentrations 0.1, 0.3, 0.2, and 0.2 mg/ml were used to treat the HN18, HN17, HN30, and HN31 cells respectively. The cell cycle and sub-G1 DNA content were analyzed in the HNSCC cell lines. Cisplatin (10 μg/ml) was used as a positive control. EEOS significantly arrested the cell cycle at the G0/G1 phase in the HN30 and HN31 cells compared with control ($p < 0.05$) (Fig. 3C and D). However, the results showed no significant difference in the cell cycle status in the EEOS-treated HN18 and HN17 cells and control ($p > 0.05$) (Fig. 3A and B). Moreover, EEOS induced DNA damage as demonstrated by a significantly increased fold change in the sub-G1 DNA content in the HN18, HN30, and HN31 cells, but not the HN17 cells, compared with control (Fig. 3E).

3.4. Effect of EEOS on apoptosis in HNSCC cells

EEOS mostly induced early apoptosis in each HNSCC cell line (Fig. 4A). The percentage of apoptotic cells significantly increased in the EEOS-treated HN18, HN30, and HN31 cells compared with control ($p < 0.05$) (Fig. 4B). In addition, some of the apoptotic cell population in the EEOS or cisplatin-treated HN30 cells was defined as late apoptosis. In contrast, EEOS did not significantly induce apoptosis in the HN17 cells compared with control ($p > 0.05$).

3.5. Alteration in caspase activation in EEOS-treated HNSCC cells

Caspase-9 and-3 are the key proteolytic enzymes in response to the activation of apoptosis. We found that EEOS significantly increased the activation fold change in caspase-9, but decreased that of caspase-3 in HN18 cells compared with control ($p < 0.05$) (Fig. 5A and B). Caspase-3 was significantly activated to a higher fold change in the EEOS-treated HN17 cells than that of the untreated cells ($p < 0.05$) (Fig. 5B). However, caspase-9 and -3 was not activated when the HN30 and HN31 cells were exposed to EEOS.
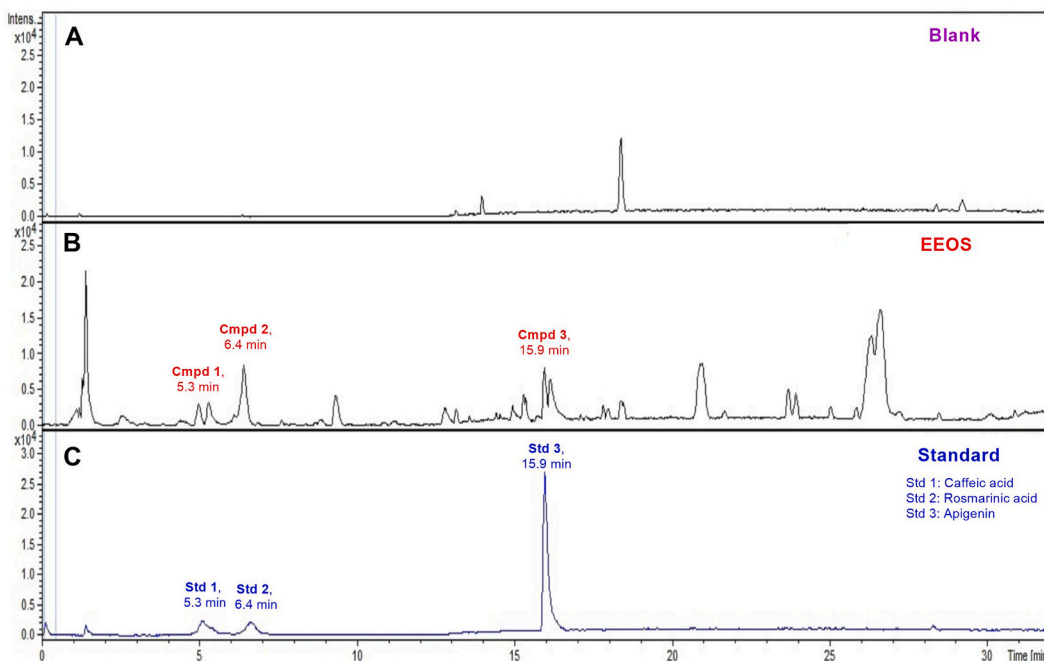
Fig. 6. HPLC-ESI-TOF-MS analysis of EEOS. Chromatogram of (A) solvent blank, (B) EEOS sample, and (C) standard compounds [caffeic acid (Std 1, 5.3 min), rosmarinic acid (Std 2, 6.4 min) and apigenin (Std 3, 15.9 min)] by negative mode HPLC-ESI-TOF-MS.

Table 1
Retention time, calculated and detected masses, calculated formula, concentration and putative identification of the three compounds in EEOS analyzed by HPLC-ESI-TOF-MS.

Compounds	Retention time (min)	Calculated $[M - H]^-$ (m/z)	Detected $[M - H]^-$ (m/z)	Calculated formula $[M - H]^-$	Concentration (µg/ml) mean ± standard deviation	Putative identification
1	5.3	179.0349	179.0353	$C_9H_7O_4$	1.89 ± 0.15	Caffeic acid
2	6.4	359.0772	359.0763	$C_{18}H_{15}O_8$	9.24 ± 0.38	Rosmarinic acid
3	15.9	269.0455	269.0461	$C_{16}H_9O_5$	0.14 ± 0.02	Apigenin

3.6. Chemical compounds analysis in EEOS

HPLC-ESI-TOF-MS was used to analyze the profiles of the polyphenolic compounds in EEOS. Commercially available polyphenolic compounds were used as standards in this study. The baseline of the HPLC system was calibrated using the sample solvent (Fig. 6A). Three compounds were detected in different quantities. The EEOS chromatograms exhibited peaks 1, 2, and 3 with retention times similar to those of caffeic acid (5.3 min), rosmarinic acid (6.4 min), and apigenin (15.9 min), respectively (Fig. 6B and C). The EEOS chemical profile was analyzed by the optimized parameters in HPLC-ESI-TOF-MS. The 3 detected compounds in EEOS were putatively identified by comparing their calculated masses and formula to the database (Table 1). The results revealed that compound 1, 2, and 3 was caffeic acid, rosmarinic acid, and apigenin, respectively. The amount of these phenolic compounds in EEOS was estimated using a calibration curve constructed using standard compounds. The quantitative determination indicated that the concentration (mean ± SD) of caffeic acid, rosmarinic acid, and apigenin in the EEOS was 1.89 ± 0.15 µg/ml, 9.24 ± 0.38 µg/ml, and 0.14 ± 0.02 µg/ml, respectively.

4. Discussion

Numerous studies indicate that specific natural bioactive substances have the potential to regulate redox balance and exhibit potential as anticancer agents. Polyphenol bioactive substances are secondary metabolites that are commonly found in plants. Among these, phenolic acids and flavonoids are the most common and abundant polyphenols. Interestingly, these compounds derived from plants found worldwide contain both antioxidant and prooxidant properties that affect cell proliferation and apoptosis [30–32]. Previous studies demonstrated that various secondary metabolites, including phenolic acid and flavonoids, were present in *O. sanctum* leaf extracts [14,33–35].

In the present study, we evaluated the anticancer effect of EEOS on 4 HNSCC cell lines. The MTT assay indicated that the extract

was cytotoxic to primary (HN18, HN30) and metastatic (HN17 and HN31) cell lines in a dose-dependent manner. Our findings imply that EEOS might have active compounds that are deleterious to HNSCC cells [33]. However, there was no significant difference in EEOS cytotoxicity between primary and metastatic cell lines based on IC$_{50}$ values. Previous studies revealed that *O. sanctum* extracts were cytotoxic to various tumors, including head and neck cancer cells [25,36], gastric cancer [20], lung adenocarcinoma cell [24], non-small cell lung carcinoma cells [37], and pancreatic cancer cells [23]. These studies are in agreement with our findings.

Studies have indicated that the anticancer effects of various treatments are closely linked with an increase in ROS concentration in cancer cells. This indicates that ROS elevation is a crucial mechanism of action and effectiveness of conventional cancer therapies, which is directly associated with cancer cell death. The mechanism underlying how elevated ROS levels affect cancer cells involves either increasing ROS production through external agents or suppressing the cellular antioxidant system [38]. The present data demonstrated up-regulation of ROS activity in response to EEOS in HN18 and HN17 cells. A previous study demonstrated the potential involvement of both ROS and RNS in the pathogenesis of HNSCC. They found that ROS and RNS enhanced lipid peroxidation and nitric oxide products and interfered with the cells' antioxidant defense system [7]. The increased ROS level during EEOS treatment might be due to its antioxidant effect [19]. Therefore, the mechanistic basis for explaining the effect of EEOS on cancer cells might involve increased ROS stress in the cancer cells [3,9]. However, EEOS had no effect on intracellular ROS levels in the HN30 and HN 31 cell lines. These findings suggest that the mechanism by which *O. sanctum* extracts have anticancer effects is complicated and not fully understand. However, our results are only partially consistent with previous studies that have shown an increase in ROS levels in lung cancer cells treated with EEOS [24,37].

Regardless of the type of ROS, the initial step in ROS-induced cellular injury involves the peroxidation of cellular membrane components, particularly membrane lipids, through a process referred to as lipid peroxidation. The products of lipid peroxidation, malondialdehyde and 4-hydroxynonenal, are suggested to be used as indicators of ROS-dependent cell and tissue damage [39]. Because ROS were induced by EEOS in HNSCC cells, we investigated the effect of this extract on membrane lipid peroxidation. In addition to the cytotoxicity and ROS findings, increased malondialdehyde production was observed in the EEOS-treated HN18 and HN31 cells compared with untreated cells. In contrast, EEOS did not induce lipid peroxidation in the HN17 and HN30 cells. It is possible that EEOS-induced excess ROS leads to cell death through various mechanisms that may not be associated with lipid peroxidation [40,41]. However, clinical studies on HNSCC have reported and highlighted increased salivary malondialdehyde levels in oral cancer patients [7,42]. This evidence may support the effect of EEOS-induced ROS on the lipid peroxidation found in our HNSCC cell lines.

We also studied how EEOS affected the cell cycle and induced DNA damage in HNSCC cells. EEOS was tested for its ability to arrest the cell cycle. We found that EEOS significantly arrested the cell cycle at the G0/G1 phase in the HN30 and HN31 cells; however, there was no effect on the cell cycle status in the HN18 and HN17 cells. Further analysis revealed that EEOS induced DNA damage in the HN18, HN30, and HN31 cells, but not the HN17 cells, compared with control. *O. sanctum* leaf extracts increased the sub-G1 population in myeloid leukemia cells [43] and lung cancer cells [44]. ROS accumulation can cause DNA damage that results in changes in the expression of the damage response downstream proteins, such as p53 and p21. The aforementioned genes have a crucial function in regulating the cellular response to different types of stress, primarily by activating or inhibiting numerous genes that control cell cycle arrest and programmed cell death [45]. Further investigation is needed to determine if EEOS-mediated cell cycle arrest is regulated by cell cycle regulators such as p53 and p21.

An apoptosis assay was conducted to determine the mechanism by which EEOS induces cytotoxicity in HNSCC cells, as it is known to be an effective approach for managing the growth of tumors. Apoptosis is a crucial mechanism for eliminating mutated or proliferating neoplastic cells from a tissue [46]. EEOS induced early apoptosis in the HN18, HN30, and HN31 cells, but not the HN17 cells. Previous studies demonstrated that *O. sanctum* leaf extracts enhanced apoptosis in myeloid leukemia cells [43], pancreatic cancer cells [23], and lung cancer cells [24,37]. Our findings expand the understanding of the apoptotic effect of *O. sanctum* leaf extracts on various types of HNSCC cell lines.

Elevated levels of ROS can interfere with the mitochondrial membrane potential, leading to the activation of the apoptosis signaling pathway through selective activation of certain caspase enzymes [38]. Therefore, caspase-9 and caspase-3 levels were analyzed in the EEOS-treated HNSCC cells in this study. However, the effect of EEOS on caspase activation in HNSCCs was not conclusive. Caspase-9 activation was observed in the EEOS-treated HN18 cells. In contrast, the caspase-3 level was decreased in this cell line. Only caspase-3 was activated in the EEOS-treated HN17 cells. Surprisingly, EEOS did not activate caspase-9 or -3 in the HN30 and HN31 cells. Our results partially support previous research which showed that treatment with ethanol extracts of *O. sanctum* leaves induced apoptosis via the activation of caspase-9 and -3 in lung cancer cells [24,44].

The initiation of ROS-mediated apoptosis can occur through two pathways, intrinsic or extrinsic. Intrinsic apoptosis is characterized by the impact of ROS on mitochondrial activity. When ROS levels rise, mitochondrial membrane potential is disrupted, which causes the release of cytochrome C. This release promotes the binding of nucleotides to apoptotic protein activating factor 1, which then activates caspase-9. Ultimately, this leads to the activation of caspase-3. In the extrinsic apoptosis pathway, elevated ROS levels activate death receptors and trigger caspase-8 to cleave caspase-3, resulting in apoptosis [30,47]. Interestingly, our results showed that caspase-3 was not activated in HN18 cells treated with EEOS, which was consistent with the apoptosis assay results. Therefore, it can be concluded that EEOS induces early apoptosis in HN18 cells through the intrinsic pathway via ROS activation, as previously reported in other studies [24,43,46].

The results of our study showed that EEOS caused apoptosis in HN30 and HN31 cells without any activation of ROS, caspase-9, or -3. This indicates that the mechanism of apoptosis induction by EEOS in these cells may be caspase-independent. Previous studies also support the possibility of caspase-independent apoptosis induced by natural compounds such as EEOS [48–51]. We observed that the apoptotic responses in the HN30 and HN31 cells were not associated with ROS, different from the conventional apoptotic mechanisms.
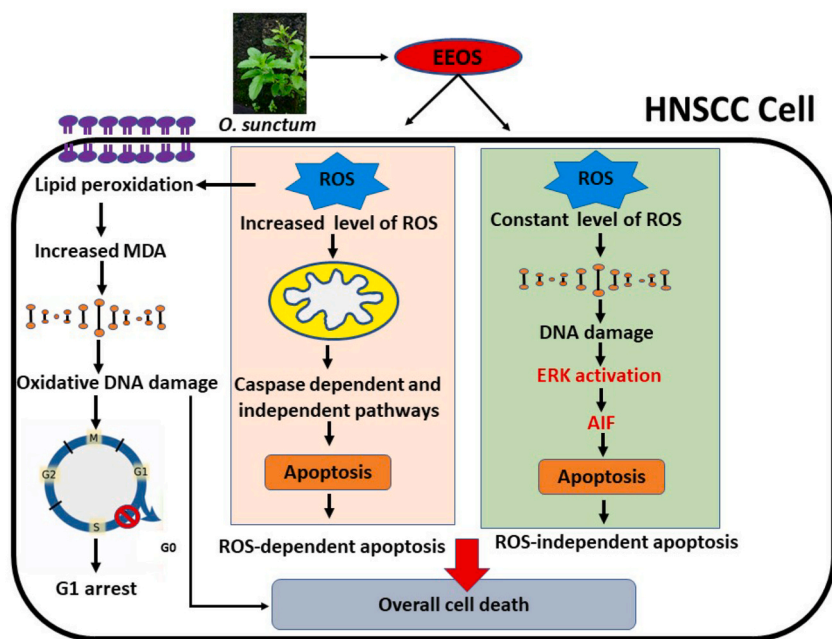
Fig. 7. The proposed mechanisms for *Ocimum sanctum* leaf extract-induced cell cycle arrest and cell death in HNSCC cells. The ethanolic extract of *O. sanctum* leaf (EEOS) increased the accumulation of intracellular Reactive Oxygen Species (ROS), which resulted in lipid peroxidation [malondialdehyde (MDA) production]. Consequently, oxidative DNA damage occurred and then the cell cycle was arrested at the G1 phase and/or cell death. EEOS induced ROS-mediated apoptosis via caspase-dependent and independent pathways. ROS-independent apoptosis was also identified in this study. EEOS might induce DNA damage and the extracellular signal-regulated kinase (ERK) activation. The activation released Apoptosis-Inducing Factor (AIF) that leads to apoptosis. In the figure, black text indicates the results from our study and the red text indicates what is already known or can be implied from a previous study [51]. (For interpretation of the references to color in this figure legend, the reader is referred to the Web version of this article.)

EEOS-induced apoptosis in the HN30 and HN31 cells may be due to ROS-independent apoptosis [52].

While caspase-3 activation is often linked to apoptosis in mammalian cells, there is growing evidence to suggest that this may not always be the case. In fact, recent research has shown that caspase-3 activation may play a role in other signaling pathways that can actually promote cell survival and proliferation [53,54]. Our results indicated that although EEOS activated caspase-3 in the HN17 cells, it did not cause apoptosis. This suggests that caspase activation induced by EEOS may not be involved in the process of apoptotic cell death [55].

The four HNSCC cell lines used in this experiment have different cellular characteristics, including tissue type [27], and cell cycle, and apoptotic responses to microenvironmental stress [56]. Our data demonstrated that EEOS modulated oxidative stress and apoptosis in different patterns between HNSCC cell lines. These results showed that EEOS caused a universal increase in intracellular ROS levels, lipid oxidation, DNA damage, cell cycle arrest, and apoptosis in all HNSCC cells. Interestingly, our study provides new insight into the apoptotic mechanism by EEOS in HNSCC cells. It should be noted that the crude extract used in this study is not composed of a single chemical compound. It is a mixture of secondary metabolites of *O. sanctum*. Polyphenolic compounds, such as caffeic acid, rosmarinic acid, and apigenin, have been identified in *O. sanctum* extracts antioxidative profiles [35] and anticancer activities [25]. In addition, these compounds were detectable in our EEOS. This implies that in future studies, caffeic acid, rosmarinic acid, and apigenin can be considered as reference compounds for the preparation of EEOS. The previous studies demonstrated that caffeic acid or apigenin induced intracellular ROS and caused DNA damage, cell cycle arrest, and apoptosis in some cancer cells, such as fibrosarcoma [57], colorectal cancer [58], and mesothelioma cells [59]. In contrast, rosmarinic acid was proposed as an anticancer compound by reducing the invasion, migration, and metastasis of lung cancer cell [60]. It remains unknown whether the anticancer effects of EEOS on HNSCC cell lines that were found in this study and a previous study [25] are due to a specific component or the additive effect of more than 1 component. Moreover, the safe dose of EEOS was not explored in this study. The complex mechanism by which EEOS induces cell cycle arrest and apoptosis in HNSCC cells is proposed in Fig. 7. An understanding of the mechanism of oxidative stress modulation is critical to understand how best to clinically develop plant-based anticancer reagents [61]. Further investigation of the mechanisms by which *O. sanctum* leaf extracts induce redox balance, cell cycle arrest, and apoptosis may provide valuable information for its use in head and neck cancer therapy. In addition, the cytotoxic effect of EEOS on normal cells needs to be investigated prior to conducting in vivo studies.

5. Conclusions

Taken together, our results demonstrated that EEOS exhibited different effects depending on the HNSCC cell type. The cytotoxic effects of EEOS on primary and metastatic HNSCC cells varied depending on the specific cell type, despite inducing increased ROS levels, lipid oxidation, DNA damage, cell cycle arrest, and apoptotic death. However, our findings provide an overview of the prooxidant and anticancer properties of EEOS by focusing on ROS dependent and independent pathways.

Author contribution statement

Kusumawadee Utispan: Conceived and designed the experiments; Performed the experiments; Analyzed and interpreted the data; Contributed reagents, materials, analysis tools or data; Wrote the paper.

Sittichai Koontongkaew, Boon-ek Yingyongnarongkul: Analyzed and interpreted the data; Contributed reagents, materials, analysis tools or data; Wrote the paper.

Nattisa Niyomtham: Performed the experiments; Analyzed and interpreted the data; Wrote the paper.

Funding statement

Data availability statement

Data will be made available on request.

Declaration of competing interest

The authors declare that they have no known competing financial interests or personal relationships that could have appeared to influence the work reported in this paper. The authors declare the following financial interests/personal relationships which may be considered as potential competing interests.

Acknowledgements

References

[1] F. Bray, J. Ferlay, I. Soerjomataram, R.L. Siegel, L.A. Torre, A. Jemal, Global cancer statistics 2018: GLOBOCAN estimates of incidence and mortality worldwide for 36 cancers in 185 countries, Ca - Cancer J. Clin. 68 (2018) 394–424.

[2] M. Arnold, M. Laversanne, L.M. Brown, S.S. Devesa, F. Bray, Predicting the future burden of esophageal cancer by histological subtype: International trends in incidence up to 2030, Am. J. Gastroenterol. 112 (2017) 1247–1255.

[3] U.S. Srinivas, B.W.Q. Tan, B.A. Vellayappan, A.D. Jeyasekharan, ROS and the DNA damage response in cancer, Redox Biol. 25 (2019) 101084.

[4] G. Huang, S.T. Pan, ROS-mediated therapeutic strategy in chemo-/radiotherapy of head and neck cancer, Oxid. Med. Cell. Longev. 2020 (2020), 5047987.

[5] H. Hwang, R. Biswas, P.S. Chung, J.C. Ahn, Modulation of EGFR and ROS induced cytochrome c release by combination of photodynamic therapy and carboplatin in human cultured head and neck cancer cells and tumor xenograft in nude mice, J. Photochem. Photobiol., B 128 (2013) 70–77.

[6] C. Sanchez-Rodriguez, R. Palao-Suay, L. Rodriganez, M.R. Aguilar, S. Martin-Saldana, J. San Roman, et al., Alpha-tocopheryl succinate-based polymeric nanoparticles for the treatment of head and neck squamous cell carcinoma, Biomolecules 8 (2018).

[7] M.H. Rasheed, S.S. Beevi, A. Geetha, Enhanced lipid peroxidation and nitric oxide products with deranged antioxidant status in patients with head and neck squamous cell carcinoma, Oral Oncol. 43 (2007) 333–338.

[8] S. Emanuele, A. D'Anneo, G. Calvaruso, C. Cernigliaro, M. Giuliano, M. Lauricella, The double-edged sword profile of redox signaling: oxidative events as molecular switches in the balance between cell physiology and cancer, Chem. Res. Toxicol. 31 (2018) 201–210.

[9] Q. Cui, J.Q. Wang, Y.G. Assaraf, L. Ren, P. Gupta, L. Wei, et al., Modulating ROS to overcome multidrug resistance in cancer, Drug Resist. Updates 41 (2018) 1–25.

[10] B. Zhang, X. Fan, Z. Wang, W. Zhu, J. Li, Alpinumisoflavone radiosensitizes esophageal squamous cell carcinoma through inducing apoptosis and cell cycle arrest, Biomed. Pharmacother. 95 (2017) 199–206.

[11] U. Kustiati, H. Wihadmadyatami, D.L. Kusindarta, Dataset of phytochemical and secondary metabolite profiling of holy basil leaf (*Ocimum sanctum* Linn) ethanolic extract using spectrophotometry, thin layer chromatography, Fourier transform infrared spectroscopy, and nuclear magnetic resonance, Data Brief 40 (2022), 107774.

[12] F. Paciello, A.R. Fetoni, D. Mezzogori, R. Rolesi, A. Di Pino, G. Paludetti, et al., The dual role of curcumin and ferulic acid in counteracting chemoresistance and cisplatin-induced ototoxicity, Sci. Rep. 10 (2020) 1063.

[13] L.S. Li, S. Reddy, Z.H. Lin, S. Liu, H. Park, S.G. Chun, et al., NQO1-mediated tumor-selective lethality and radiosensitization for head and neck cancer, Mol. Cancer. Ther. 15 (2016) 1757–1767.

[14] M.S. Baliga, R. Jimmy, K.R. Thilakchand, V. Sunitha, N.R. Bhat, E. Saldanha, et al., *Ocimum sanctum* L (holy basil or tulsi) and its phytochemicals in the prevention and treatment of cancer, Nutr. Cancer 65 (2013) 26–35.

[15] F. Bast, P. Rani, D. Meena, Chloroplast DNA phylogeography of holy basil (*Ocimum tenuiflorum*) in Indian subcontinent, Sci. World J. (2014), 847482.

[16] T. Suanarunsawat, G. Anantasomboon, C. Piewbang, Anti-diabetic and anti-oxidative activity of fixed oil extracted from *Ocimum sanctum* L. leaves in diabetic rats, Exp. Ther. Med. 11 (2016) 832–840.

[17] P. Bhattacharyya, A. Bishayee, *Ocimum sanctum* Linn. (Tulsi): an ethnomedicinal plant for the prevention and treatment of cancer, Anti Cancer Drugs 24 (2013) 659–666.

[18] S.K. Gupta, J. Prakash, S. Srivastava, Validation of traditional claim of Tulsi, *Ocimum sanctum* Linn. as a medicinal plant, Indian J. Exp. Biol. 40 (2002) 765–773.

[19] M.A. Kelm, M.G. Nair, G.M. Strasburg, D.L. DeWitt, Antioxidant and cyclooxygenase inhibitory phenolic compounds from *Ocimum sanctum* Linn, Phytomedicine 7 (2000) 7–13.

[20] P. Manikandan, P. Vidjaya Letchoumy, D. Prathiba, S. Nagini, Proliferation, angiogenesis and apoptosis-associated proteins are molecular targets for chemoprevention of MNNG-induced gastric carcinogenesis by ethanolic *Ocimum sanctum* leaf extract, Singapore Med. J. 48 (2007) 645–651.

[21] T. Manaharan, R. Thirugnanasampandan, R. Jayakumar, G. Ramya, G. Ramnath, M.S. Kanthimathi, Antimetastatic and anti-inflammatory potentials of essential oil from edible *Ocimum sanctum* leaves, Sci. World J. 2014 (2014), 239508.

[22] P. Eswar, C.G. Devaraj, P. Agarwal, Anti-microbial activity of Tulsi {*Ocimum Sanctum* (Linn.)} extract on a periodontal pathogen in human dental plaque: an in vitro study, J. Clin. Diagn. Res. 10 (2016) ZC53–56.

[23] T. Shimizu, M.P. Torres, S. Chakraborty, J.J. Souchek, S. Rachagani, S. Kaur, et al., Holy basil leaf extract decreases tumorigenicity and metastasis of aggressive human pancreatic cancer cells in vitro and in vivo: potential role in therapy, Cancer Lett. 336 (2013) 270–280.

[24] H. Wihadmadyatami, S. Karnati, P. Hening, Y. Tjahjono, Rizal, F. Maharjanti, et al., Ethanolic extract *Ocimum sanctum* Linn. induces an apoptosis in human lung adenocarcinoma (A549) cells, Heliyon 5 (2019), e02772.

[25] K. Utispan, N. Niyomtham, B.E. Yingyongnarongkul, S. Koontongkaew, Ethanolic Extract of *Ocimum sanctum* leaves reduced invasion and matrix metalloproteinase activity of head and neck cancer cell lines, Asian Pac. J. Cancer Prev. 21 (2020) 363–370.

[26] A.M. Luke, R. Patnaik, S.T. Kuriadom, M. Jaber, S. Mathew, An in vitro study of *Ocimum sanctum* as a chemotherapeutic agent on oral cancer cell-line, Saudi J. Biol. Sci. 28 (2021) 887–890.

[27] M. Cardinali, H. Pietraszkiewicz, J.F. Ensley, K.C. Robbins, Tyrosine phosphorylation as a marker for aberrantly regulated growth-promoting pathways in cell lines derived from head and neck malignancies, Int. J. Cancer 61 (1995) 98–103.

[28] K. Utispan, S. Koontongkaew, Macrophage migration inhibitory factor modulates proliferation, cell cycle, and apoptotic activity in head and neck cancer cell lines, J. Dent. Sci. 16 (2021) 342–348.

[29] P. Mishra, C.M. Pandey, U. Singh, A. Gupta, C. Sahu, A. Keshri, Descriptive statistics and normality tests for statistical data, Ann. Card Anaesth. 22 (2019) 67–72.

[30] S. NavaneethaKrishnan, J.L. Rosales, K.Y. Lee, ROS-mediated cancer cell killing through dietary phytochemicals, Oxid. Med. Cell. Longev. 2019 (2019), 9051542.

[31] S. Miccadei, D. Di Venere, A. Cardinali, F. Romano, A. Durazzo, M.S. Foddai, et al., Antioxidative and apoptotic properties of polyphenolic extracts from edible part of artichoke (*Cynara scolymus* L.) on cultured rat hepatocytes and on human hepatoma cells, Nutr. Cancer 60 (2008) 276–283.

[32] H. Luo, A. Yang, B.A. Schulte, M.J. Wargovich, G.Y. Wang, Resveratrol induces premature senescence in lung cancer cells via ROS-mediated DNA damage, PLoS One 8 (2013), e60065.

[33] R. Borah, S.P. Biswas, Tulsi (*Ocimum sanctum*), excellent source of phytochemicals, Int J Environ Agri Biotech 3 (2018) 1732–1738.

[34] S. Ullah, K.U. Rahman, K.U. Rahman, A. Hussain, A.H. Ramadan, Phenolic acids, flavenoids and antiradical activity of *Ocimum sanctum* and *Ocimum basilicium* leaves extract, J Med Spice Plants 24 (2020) 60–62.

[35] A. Chaudhary, S. Sharma, A. Mittal, S. Gupta, A. Dua, Phytochemical and antioxidant profiling of *Ocimum sanctum*, J. Food Sci. Technol. 57 (2020) 3852–3863.

[36] P. Shivpuje, R. Ammanangi, K. Bhat, S. Katti, Effect of *Ocimum sanctumon* oral cancer cell line: an in vitro study, J. Contemp. Dent. Pract. 16 (2015) 709–714.

[37] M. Sridevi, B. John, K. Yamini, Anti-cancer effect of *Ocimum sanctum* ethanolic extract in non-small cell lung carcinoma cell line, Int J Pharm Sci 8 (2016) 242–246.

[38] V. Aggarwal, H.S. Tuli, A. Varol, F. Thakral, M.B. Yerer, K. Sak, et al., Role of reactive oxygen species in cancer progression: molecular mechanisms and recent advancements, Biomolecules 9 (2019).

[39] S. Kwiecien, K. Jasnos, M. Magierowski, Z. Sliwowski, R. Pajdo, B. Brzozowski, et al., Lipid peroxidation, reactive oxygen species and antioxidative factors in the pathogenesis of gastric mucosal lesions and mechanism of protection against oxidative stress-induced gastric injury, J. Physiol. Pharmacol. 65 (2014) 613–622.

[40] L. He, T. He, S. Farrar, L. Ji, T. Liu, X. Ma, Antioxidants maintain cellular redox homeostasis by elimination of reactive oxygen species, Cell. Physiol. Biochem. 44 (2017) 532–553.

[41] Z. Wang, T. Xia, S. Liu, Mechanisms of nanosilver-induced toxicological effects: more attention should be paid to its sublethal effects, Nanoscale 7 (2015) 7470–7481.

[42] S.R. Shetty, S. Babu, S. Kumari, P. Shetty, S. Hegde, R. Castelino, Status of salivary lipid peroxidation in oral cancer and precancer, Indian J. Med. Paediatr. Oncol. 35 (2014) 156–158.

[43] A. Haldar, N. Deb, S. Besra, Induction of apoptosis by *Ocimum sanctum* (Holy basil) leaf extract against myeloid leukemia cells, Int. J. Biosci. 17 (2020) 194–206.

[44] V. Magesh, J.C. Lee, K.S. Ahn, H.J. Lee, H.J. Lee, E.O. Lee, et al., *Ocimum sanctum* induces apoptosis in A549 lung cancer cells and suppresses the in vivo growth of Lewis lung carcinoma cells, Phytother Res. 23 (2009) 1385–1391.

[45] X. Zhu, K. Wang, K. Zhang, B. Huang, J. Zhang, Y. Zhang, et al., Ziyuglycoside II inhibits the growth of human breast carcinoma MDA-MB-435 cells via cell cycle arrest and induction of apoptosis through the mitochondria dependent pathway, Int. J. Mol. Sci. 14 (2013) 18041–18055.

[46] S. Elmore, Apoptosis: a review of programmed cell death, Toxicol. Pathol. 35 (2007) 495–516.

[47] M. Redza-Dutordoir, D.A. Averill-Bates, Activation of apoptosis signalling pathways by reactive oxygen species, Biochim. Biophys. Acta 1863 (2016) 2977–2992.

[48] R. Kim, M. Emi, K. Tanabe, Caspase-dependent and -independent cell death pathway after DNA damage (Review), Oncol. Rep. 14 (2005) 595–599.

[49] I. Mathiasen, M. Jaattela, Triggering caspase-independent cell death. to combat cancer, Trends Mol. Med. 8 (2002) 212–220.

[50] W. Fiers, R. Beyaert, W. Declereg, P. Vandenabeele, More than one way to die: apoptosis, necrosis and reactive oxygen damage, Oncogene 18 (1999) 7719–7730.

[51] T.D. Singh, H.T. Meitei, A.L. Sharma, A. Robinson, L.S. Singh, T.R. Singh, Anticancer properties and enhancement of therapeutic potential of cisplatin by leaf extract of *Zanthoxylum armatum* DC, Biol. Res. 48 (2015) 46.

[52] D.X. Hou, T. Uto, X. Tong, T. Takeshita, S. Tanigawa, I. Imamura, et al., Involvement of reactive oxygen species-independent mitochondrial pathway in gossypol-induced apoptosis, Arch. Biochem. Biophys. 428 (2004) 179–187.

[53] L. Broker, F. Kruyt, G. Giaccone, Cell death independent of caspases: a review, Clin. Cancer Res. 11 (2005) 3155–3162.

[54] J. Perfettini, G. Kroemer, Caspase activation is not death, Nat. Immunol. 4 (2003) 308–310.

[55] S.Y. Yang, S. Bolvin, K.M. Sales, B. Fuller, A.M. Seifalian, M.C. Winslet, IGF-I activates caspases 3/7, 8 and 9 but does not induce cell death in colorectal cancer cells, BMC Cancer 9 (2009) 158.

[56] K. Utispan, S. Koontongkaew, High nitric oxide adaptation in isogenic primary and metastatic head and neck cancer cells, Anticancer Res. 40 (2020) 2657–2665.

[57] N. Rajendra Prasad, A. Karthikeyan, S. Karthikeyan, B.V. Reddy, Inhibitory effect of caffeic acid on cancer cell proliferation by oxidative mechanism in human HT-1080 fibrosarcoma cell line, Mol. Cell. Biochem. 349 (2011) 11–19.

[58] K. Banerjee, M. Mandal, Oxidative stress triggered by naturally occurring flavone apigenin results in senescence and chemotherapeutic effect in human colorectal cancer cells, Redox Biol. 5 (2015) 153–162.

[59] Y.J. Lee, K.S. Park, H.S. Nam, M.K. Cho, S.H. Lee, Apigenin causes necroptosis by inducing ROS accumulation, mitochondrial dysfunction, and ATP depletion in malignant mesothelioma cells, Korean J. Physiol. Pharmacol. 24 (2020) 493–502.

[60] K. Pintha, W. Chaiwangyen, S. Yodkeeree, M. Suttajit, P. Tantipaiboonwong, Suppressive effects of rosmarinic acid rich fraction from perilla on oxidative stress, inflammation and metastasis ability in A549 cells exposed to PM via C-Jun, P-65-Nf-Kappab and Akt signaling pathways, Biomolecules (2021) 11.

[61] P. Rijo, M. Pesic, A.S. Fernandes, C.N. Santos, Natural products: optimizing cancer treatment through modulation of redox balance, Oxid. Med. Cell. Longev. 2020 (2020), 2407074.